Acta Crystallographica Section B
Structural Science
ISSN 0108-7681

42 salt forms of tyramine: structural comparison and the occurrence of hydrate formation

Naomi E. B. Briggs, Alan R. Kennedy* and Catriona A. Morrison*

WestCHEM, Department of Pure and Applied Chemistry, University of Strathclyde, Glasgow G1 1XL, Scotland

Correspondence e-mail: a.r.kennedy@strath.ac.uk, catriona.morrison@strath.ac.uk

Received 20 April 2012
Accepted 11 June 2012

The single-crystal diffraction structures of 38 salt forms of the base tyramine (4-hydroxyphenethylamine) are reported for the first time. Together with literature examples, these structures are discussed with respect to cation conformation, cation packing, hydrogen bonding and hydrate formation. It is found that isostructural cation packing can occur even with structurally different anions, with different hydration states and with different hydrogen bonding. Hydrate formation is found to be more likely both (i) when there is an increase in the total number of potential hydrogen bond acceptor and donor atoms; and (ii) when the ratio of potential hydrogen bond donor to acceptor atoms is low.

1. Introduction

Using the salt form of a drug is one of the simplest and commonest ways to manipulate the physicochemical properties of the drug without significantly altering the desirable molecular features of the active pharmaceutical ingredient (API; Stahl & Wermuth, 2008; Gould, 1986). If the relevant structure–property relationships were fully understood then selecting the correct salt form to give a desired property (such as a specific solubility, melting point or hygroscopicity) should be an exercise in logic. However, these relationships are poorly understood. A contributing factor is that understanding structure–property relationships requires the availability of relatively large and systematic series of structures of relevant salt forms, and such series are rare. Of such datasets that do exist (Black *et al.*, 2007; Collier *et al.*, 2006; Kennedy *et al.*, 2011; Lewis *et al.*, 2005) two are of phenylethylamine (PEA) based drugs. The PEA family includes pharmaceutically significant compounds such as the decongestant ephedrine, the anti-asthma drug salbutamol and the stimulant methamphetamine. The current paper adds to this by describing a dataset of 42 structures of salt forms of tyramine (4-hydroxyphenethylamine, see Scheme 1), a PEA that occurs naturally in foodstuffs and which has been identified as a neurotransmitter and implicated in the occurrence of migraine clusters (Siddiqui *et al.*, 2009; D'Andrea *et al.*, 2007). The structures will be discussed in terms of conformation of the tyrammonium cation, hydrogen-bond formation and crystal packing similarities with the latter investigated with regard to cation packing through analysis of an isostructural tree. The occurrence of hydrate formation is also examined.

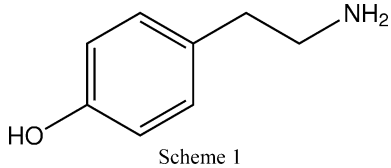

Scheme 1

The latter point is important as hydrates can differ substantially in their physicochemical properties compared with their equivalent anhydrous form (Grant & Higuchi, 1990). As water is the solvent of choice or of necessity for many processes involving APIs, APIs are brought into contact with water during many of the drug development stages, such as crystallization, or may simply be exposed to water through storage in humid atmospheres (Khankari & Grant, 1995). Examples of the detrimental effects of API hydrate formation can be found in the literature (*e.g.* Kiang *et al.*, 2009; Shankland *et al.*, 2001). Hydrated crystals can be classified in various ways (Vippagunta *et al.*, 2001; Morris, 2009). A common scheme is to use three categories, where class I hydrates (isolated site hydrates) are stoichiometric, class II hydrates (channel or planar hydrates) are non-stoichiometric and class III hydrates (ion-coordinated hydrates) may fit into either category. In pharmaceutical hydrates, water molecules usually occupy definite positions within the crystal lattice and usually form hydrogen bonds to the host molecules or ions, although many exceptions are known (see for example Kennedy *et al.*, 2003). It is thought that inclusion of water molecules in the crystal array often allows for more idealized hydrogen-bond geometries and therefore lower lattice energies (Infantes *et al.*, 2003). With respect to aqueous solubility, as the solid hydrated compound already features interactions between water and the API, the free energy that is released on dissolution is less than that seen for the equivalent anhydrous compound (Grant & Higuchi, 1990). Thus, theory predicts that the anhydrous form of a compound should always have a greater aqueous solubility than the corresponding hydrate, when both are subject to the same conditions.

Several studies have been made of organic hydrates present in crystallographic databases to try and ascertain what features result in likely hydrate formation (Infantes *et al.*, 2003; Gillon *et al.*, 2003; Görbitz & Hersleth, 2000; Infantes & Motherwell, 2002; Haynes *et al.*, 2005; Clarke *et al.*, 2010). Of these, Infantes & Motherwell (2002) reported that 6.6% of the organic entries within the Cambridge Structural Database (CSD) were hydrates and 14% of bioactive compounds were hydrates. This percentage is greatly increased when looking solely at salt compounds. For example, the study by Haynes *et al.* (2005) investigated hydrate formation in NH^+-containing salts of pharmaceutically acceptable counterions and found that hydrates were present in 22.5% of such CSD entries. It is also known that those metal cations (Na, K, Mg, Ca) commonly used as salt formers in the pharmaceutical industry typically precipitate from aqueous solution as polyhydrates (for example, Arlin *et al.*, 2011; Kennedy *et al.*, 2004, 2009). Indeed, hydrate formation is one of the major reasons why the otherwise adventitious sodium salt may not be the chosen commercial form of acidic APIs (Stahl, 1980). Similar prior knowledge about other counterions and their tendency to form hydrates would be helpful. Thus, the work presented here examines the likelihood of hydrate formation for salts of tyramine. In particular, the formation of hydrates will be investigated in terms of counterion type and hydrogen-bond donor:acceptor ratios.

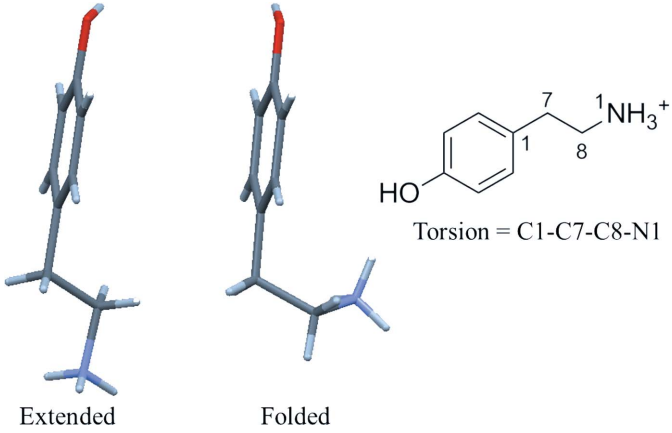

Figure 1
Two different conformations are found for the tyrammonium cation. On the left is the extended conformation, here from the 2FB salt, and on the right is the folded variant as exemplified here from the Adp2 salt structure.

2. Experimental

2.1. Salt synthesis and crystallization

All experiments were carried out using commercially available materials and all salts were prepared by the following method. A 10% excess of the selected acid was added to a partially dissolved aqueous slurry of the free base tyramine. To avoid immediate deposition of solids, additional water was added where appropriate. The resulting solution was stirred for 30 min and heated to 323 K. The solution was then filtered and left to produce crystals by slow evaporation and cooling. Where unsatisfactory single crystals were obtained, the solids were redissolved in the minimum quantity of water and the resultant solution filtered into a narrow tube of approximate diameter 5 mm, to allow for slower evaporation and crystal growth.

2.2. Crystallographic data collection and processing

Measurements on most samples were recorded at low temperature by Gemini or Xcalibur Oxford Diffraction diffractometers with graphite-monochromated Mo $K\alpha$ (λ = 0.71073 Å). Data was processed, scaled and corrected by the *CrysAlis Pro* software (Oxford Diffraction, 2006). Measurements on the 4-nitrobenzoate (4NB) crystals were made with synchrotron radiation at station I19 of the Diamond Light Source. The synchrotron X-ray wavelength was 0.6889 Å and data was collected using a Crystal Logics κ-geometry diffractometer and a Rigaku Saturn 724+ CCD detector. *CrystalClear* was used to record images (Rigaku Corporation, 2008) and the data was then transformed to Bruker format to allow processing *via SAINT* and *SADABS* (Bruker, 2007; Sheldrick, 2008). Measurements on the dihydrogenphosphate,

4-chlorobenzoate, 4-nitrobenzoate, hydrogen maleate and racemic hydrogen tartrate salts (HPO, 4CB, 4NB, Male and RTar) were made by the National Crystallography Service (Cole & Gale, 2012). Structure solution used programs from the *SHELXS* or *SIR* families (Sheldrick, 2008; Altomare *et al.*, 1994, 1999). Refinement of non-H atoms was with anisotropic displacement parameters, was to convergence and was by the full-matrix least-squares method on F^2, as implemented by *SHELX*97 (Sheldrick, 2008) within the *WinGX* interface (Farrugia, 1997). All H atoms attached to C atoms were placed in geometric positions and refined in riding modes. Where possible, H atoms of common hydrogen-bonding groups (*e.g.* OH and NH) were placed as found by difference synthesis and refined freely. However, where this was not possible suitable restraints were used. All structures have been checked with *PLATON* (Spek, 2003) and the *checkCIF* routine available from the IUCr website. Molecular graphics were prepared using *Mercury* (Macrae *et al.*, 2008). Selected crystallographic and refinement parameters are given in Table 1 and full details are available as supplementary files.[1]

3. Results and discussion

Salt synthesis was attempted with tyramine and the 42 acids shown in Scheme 2. In 40 cases crystals of a desired product were grown and examined. From the reaction with adipic acid, two separate forms were recorded, one a salt and one a co-crystal of a salt. A co-crystal-containing salt was also isolated instead of a simple salt with the fumarate counterion. In two cases no suitable crystals of salt forms were obtained for analysis. These were the reaction with 2-hydroxybenzoic acid, which gave only the starting acid as a crystalline product, and the reaction with 3-aminobenzoic acid, which gave no crystals suitable for analysis. These four exceptional reactions noted above all involve carboxylic acid groups, but there appears to be little other connection between them on the grounds of shape and/or electronic effects (including pK_a). Four simple salt structures of tyramine have been described previously in the literature. These are the chloride (Podder *et al.*, 1979), the iodide (Ivanova & Spiteller, 2010), the sulfate (Koleva *et al.*, 2008) and an anhydrous phase of the dihydrogenphosphate (Kolev *et al.*, 2009). For the structural comparisons below, the chloride, sulfate and anhydrous dihydrogenphosphate structures were used as recovered from the CSD. We thus present 38 new structures and examine and compare a total of 42 crystal structures.

[1] Supplementary data for this paper are available from the IUCr electronic archives (Reference: RY5045). Services for accessing these data are described at the back of the journal.

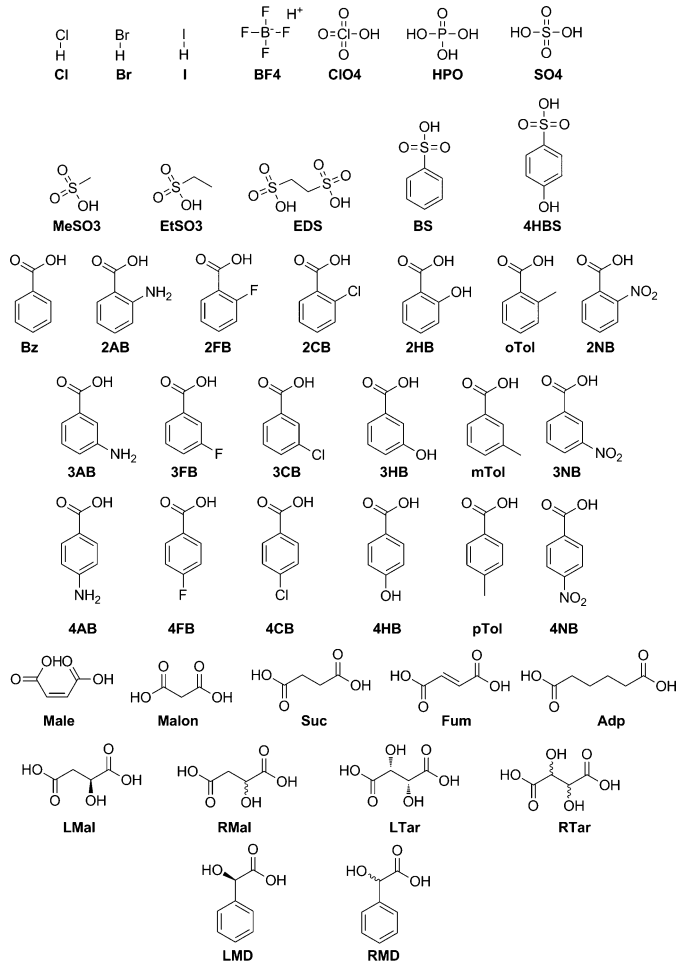

Scheme 2

3.1. Conformation of the cation

The tyramine cation is found to adopt two different conformations, one where the ethylammonium aliphatic backbone is extended and the other where it folds back towards the aryl ring. These two different conformations can be largely defined by the C1—C7—C8—N1 torsion angle, as illustrated in Fig. 1. The extended conformation is by far the most common occurring exclusively in 37 of the salt structures with a torsion angle range of 169.2 (2)° in the iodide salt to −172.3 (9)° in the *p*-toluate salt. This corresponds to having the bulky aromatic and NH_3 groups in mutually *anti* positions. The much less common folded structure occurs in only four structures, with the magnitude of these torsion angles ranging from 61.4 (2)° for the adipate monohydrate salt to 67.6 (7)° for one of the crystallographically unique cations in the 4-nitrobenzoate salt. The *m*-toluate salt is unique as it is the only structure that contains two crystallographically independent cations that adopt different cation conformations, with one extended and one folded cation per asymmetric unit. Related work on ephedrine salts found two cation conformations (Collier *et al.*, 2006; Duddu & Grant, 1994; Li *et al.*, 2001) and work on methylephedrine salts found three cation conformations (Kennedy *et al.*, 2011).

Table 1
Selected crystallographic data and refinement parameters.

$R = R[F^2 > 2\sigma(F^2)]$, $wR = wR(F^2)$, NV = No. of parameters.

Label	Chemical formula, M_r	Space group, T (K)	Cell parameters (Å, °), V (Å^3), Z	θ_{max} (°), R_{int}, $(\sin\theta/\lambda)_{max}$ (Å^{-1})	R, wR, S, N_{refl}, NV
Br	$C_8H_{12}BrNO$, 218.10	*Pbcn*, 123	a = 20.1430 (11), b = 10.9691 (4), c = 8.2747 (4), $\alpha = \beta = \gamma$ = 90, 1828.30 (15), 8	27.5, 0.031, 0.650	0.023, 0.053, 0.90, 2094, 118
I	$C_8H_{12}INO$, 265.09	$P2_12_12_1$, 123	a = 5.1194 (2), b = 9.0278 (2), c = 20.1089 (6), $\alpha = \beta = \gamma$ = 90, 929.37 (5), 4	27.98, 0.021, 0.660	0.018, 0.035, 0.98, 2061, 118
BF4	$C_8H_{14}BF_4NO_2$, 243.01	*Pbca*, 123	a = 11.9981 (7), b = 7.2291 (5), c = 24.6145 (13), $\alpha = \beta = \gamma$ = 90, 2135.0 (2), 8	27.49, 0.038, 0.649	0.039, 0.093, 0.99, 2452, 169
ClO4	$C_8H_{14}ClNO_6$, 255.65	$P2_1/c$, 123	a = 7.3939 (3), b = 25.1222 (11), c = 11.6847 (4), β = 90.896 (3), 2170.18 (15), 8	27.5, 0.057, 0.650	0.050, 0.114, 0.91, 4947, 326
HPO	$C_8H_{18}NO_7P$, 271.20	*Pbca*, 120	a = 11.0446 (9), b = 8.0666 (5), c = 29.755 (2), $\alpha = \beta = \gamma$ = 90, 2651.0 (3), 8	26.0, 0.059, 0.617	0.071, 0.153, 1.14, 2436, 191
MeSO3	$C_9H_{15}NO_4S$, 233.28	$P2_12_12_1$, 123	a = 5.0262 (1), b = 10.0739 (2), c = 21.7126 (5), $\alpha = \beta = \gamma$ = 90, 1099.38 (4), 4	27.5, 0.028, 0.650	0.027, 0.055, 0.97, 2526, 154
EtSO3	$C_{10}H_{17}NO_4S$, 247.31	$P2_1/c$, 123	a = 10.4454 (2), b = 20.6788 (3), c = 10.8374 (2), β = 91.198 (2), 2340.35 (7), 8	25.99, 0.025, 0.617	0.032, 0.069, 0.85, 4591, 332
EDS	$C_9H_{14}NO_4S$, 232.27	*Pbca*, 123	a = 9.5614 (3), b = 9.5543 (3), c = 22.7766 (7), $\alpha = \beta = \gamma$ = 90, 2080.70 (11), 8	27.49, 0.030, 0.649	0.031, 0.076, 0.95, 2375, 152
BS	$C_{14}H_{19}NO_5S$, 313.36	$P2_12_12_1$, 123	a = 7.7244 (2), b = 11.1889 (2), c = 17.4253 (4), $\alpha = \beta = \gamma$ = 90, 1506.03 (6), 4	26.0, 0.021, 0.617	0.032, 0.073, 1.05, 2705, 214
4HBS	$C_{28}H_{36}N_2O_{11}S_2$, 320.36	$P2_12_12_1$, 123	a = 7.6261 (5), b = 34.974 (2), c = 10.9159 (6), $\alpha = \beta = \gamma$ = 90, 2911.4 (3), 8	25.99, 0.071, 0.617	0.039, 0.048, 0.75, 3181, 402
Bz	$C_{15}H_{17}NO_3$, 259.30	$P2_1$, 123	a = 10.8685 (3), b = 12.0279 (2), c = 11.0849 (3), β = 110.752 (3), 1355.06 (6), 4	26.99, 0.018, 0.639	0.029, 0.065, 1.02, 5818, 375
2AB	$C_{15}H_{18}N_2O_3$, 274.31	$P2_1c$, 123	a = 10.8086 (3), b = 7.7675 (2), c = 16.3408 (5), β = 93.829 (2), 1368.84 (7), 4	27.0, 0.024, 0.639	0.035, 0.080, 1.03, 2975, 205
2FB	$C_{15}H_{16}FNO_3$, 277.29	$P2_1$, 123	a = 10.9819 (8), b = 12.2053 (6), c = 10.9963 (8), β = 111.243 (8), 1373.77 (16), 4	25.99, 0.021, 0.617	0.035, 0.063, 0.85, 3801, 369
2CB	$C_{15}H_{16}ClNO_3$, 293.75	$P2_1/c$, 123	a = 11.2539 (11), b = 12.4279 (10), c = 11.6172 (11), β = 116.306 (12), 1456.5 (2), 4	28.88, 0.066, 0.680	0.049, 0.082, 0.92, 3412, 193
oTol	$C_{16}H_{19}NO_3$, 273.32	$P2_1/c$, 123	a = 11.4527 (8), b = 12.2496 (5), c = 11.6217 (8), β = 116.740 (9), 1456.06 (15), 4	28.84, 0.032, 0.679	0.039, 0.083, 0.88, 3470, 199
2NB	$C_{15}H_{16}N_2O_5$, 304.30	$C2/c$, 123	a = 47.614 (6), b = 5.1616 (5), c = 25.552 (2), β = 96.136 (11), 6243.8 (11), 16	27.0, 0.094, 0.639	0.043, 0.103, 0.84, 6821, 418
3FB	$C_{15}H_{16}FNO_3$, 277.29	$P2_1/c$, 123	a = 11.4897 (4), b = 11.4386 (3), c = 10.8605 (3), β = 107.525 (4), 1361.10 (7), 4	27.5, 0.026, 0.650	0.036, 0.088, 0.95, 3107, 197
3CB	$C_{15}H_{16}ClNO_3$, 293.74	$C2/c$, 123	a = 24.856 (9), b = 8.1013 (9), c = 19.464 (7), β = 133.43 (6), 2846.1 (14), 8	29.46, 0.045, 0.692	0.046, 0.121, 1.02, 3530, 194
3HB	$C_{15}H_{17}NO_4$, 275.30	$P\bar{1}$, 123	a = 8.1593 (10), b = 8.7185 (9), c = 10.6386 (11), α = 85.706 (8), β = 76.200 (9), γ = 63.787 (11), 658.96 (13), 2	26.99, 0.021, 0.639	0.037, 0.086, 0.94, 2874, 201
mTol	$C_{16}H_{19}NO_3$, 273.32	$P2_1/c$, 123	a = 12.8638 (3), b = 18.4891 (4), c = 12.5939 (2), β = 97.301 (2), 2971.05 (11), 8	27.0, 0.027, 0.639	0.044, 0.110, 0.99, 6476, 395
3NB	$C_{15}H_{16}N_2O_5$, 304.30	$P2_1/c$, 123	a = 10.4944 (4), b = 11.5920 (5), c = 12.0885 (5), β = 93.465 (4), 1467.89 (10), 4	27.0, 0.019, 0.639	0.033, 0.085, 1.03, 3205, 215
4AB	$C_{15}H_{18}N_2O_3$, 274.31	$P2_1/c$, 123	a = 11.5082 (3), b = 11.2844 (3), c = 10.9033 (3), β = 107.037 (3), 1353.80 (6), 4	27.0, 0.021, 0.639	0.040, 0.096, 1.03, 2943, 205

Table 1 (continued)

Label	Chemical formula, M_r	Space group, T (K)	Cell parameters (Å, °), V (Å^3), Z	θ_{max} (°), R_{int}, $(\sin\theta/\lambda)_{max}$ (Å^{-1})	R, wR, S, N_{refl}, NV
4FB	$C_{15}H_{16}FNO_3$, 277.29	$P2_1/c$, 123	a = 11.9993 (19), b = 11.3322 (18), c = 10.7542 (18), β = 109.754 (19), 1376.3 (4), 4	27.0, 0.071, 0.639	0.038, 0.064, 0.75, 2999, 197
4CB	$C_{15}H_{16}ClNO_3$, 293.74	$P\bar{1}$, 120	a = 15.8566 (4), b = 17.5993 (4), c = 22.0881 (3), α = 105.676 (1), β = 96.763 (1), γ = 99.335 (1), 5770.8 (2), 16	27.0, 0.092, 0.639	0.101, 0.265, 1.11, 25 155, 1458
4HB	$C_{15}H_{17}NO_4$, 275.30	$P\bar{1}$, 123	a = 9.9745 (2), b = 15.1624 (4), c = 18.6406 (4), α = 76.300 (2), β = 86.480 (2), γ = 84.892 (2), 2725.70 (11), 8	27.0, 0.030, 0.639	0.036, 0.079, 0.89, 11 800, 807
pTol	$C_{16}H_{19}NO_3$, 273.32	$P2_1/c$, 123	a = 11.4797 (3), b = 11.3596 (2), c = 11.0501 (3), β = 104.932 (2), 1392.33 (6), 4	29.14, 0.022, 0.685	0.035, 0.093, 1.10, 3418, 195
4NB	$C_{15}H_{16}N_2O_5$, 304.30	$P2_1/c$, 120	a = 7.0796 (10), b = 6.1784 (14), c = 67.751 (7), β = 92.518 (6), 2960.6 (9), 8	26.0, 0.082, 0.636	0.089, 0.308, 1.09, 5466, 402
Male	$C_{12}H_{15}NO_5$, 253.25	$P2_1/c$, 120	a = 7.6924 (3), b = 5.6856 (2), c = 27.9377 (8), β = 103.047 (2), 1190.34 (7), 4	27.62, 0.047, 0.652	0.042, 0.124, 1.09, 2720, 184
Malon	$C_{11}H_{15}NO_5$, 241.24	$P2_1/c$, 123	a = 13.3025 (2), b = 7.8609 (1), c = 11.3441 (2), β = 106.174 (2), 1139.30 (3), 4	28.0, 0.015, 0.661	0.031, 0.088, 1.09, 2745, 173
Fum cocryst	$C_{24}H_{34}N_2O_{12}$, 542.54	$P\bar{1}$, 123	a = 8.8784 (4), b = 8.9774 (4), c = 9.4687 (5), α = 116.911 (5), β = 97.833 (4), γ = 91.099 (4), 663.90 (5), 1	26.98, 0.025, 0.638	0.033, 0.079, 0.96, 2899, 200
Suc	$C_{20}H_{32}N_2O_8$, 428.48	$P2_1/c$, 123	a = 11.4936 (5), b = 7.5497 (3), c = 12.5154 (8), β = 99.865 (5), 1069.94 (9), 2	26.0, 0.041, 0.617	0.035, 0.066, 0.84, 2099, 160
Adp	$C_{22}H_{36}N_2O_8$, 456.52	$P2_1/n$, 123	a = 8.6247 (3), b = 15.1897 (6), c = 8.7588 (3), β = 93.826 (3), 1144.90 (7), 2	27.0, 0.023, 0.639	0.039, 0.092, 1.04, 2498, 169
Adp·(HAdp)	$C_{28}H_{43}N_2O_{10.50}$, 575.64	$P2_1/c$, 123	a = 21.1097 (18), b = 5.9615 (4), c = 24.6027 (19), β = 105.911 (8), 2977.5 (4), 4	27.0, 0.111, 0.639	0.097, 0.179, 1.28, 6507, 423
LMal	$C_{20}H_{32}N_2O_9$, 444.48	$P2_1$, 123	a = 11.8909 (6), b = 7.7956 (4), c = 11.9547 (6), β = 100.160 (5), 1090.78 (10), 2	26.0, 0.020, 0.617	0.034, 0.077, 0.96, 4027, 340
RMal	$C_{12}H_{19}NO_7$, 289.28	$Pna2_1$, 123	a = 7.6360 (3), b = 30.0364 (13), c = 6.2787 (2), α = β = γ = 90, 1440.07 (10), 4	26.0, 0.022, 0.617	0.030, 0.059, 0.90, 2132, 213
LTar	$C_{20}H_{32}N_2O_{10}$, 460.48	$P2_1$, 123	a = 11.6895 (3), b = 7.7596 (2), c = 12.3238 (3), β = 100.013 (2), 1100.81 (5), 2	27.0, 0.019, 0.639	0.028, 0.068, 1.05, 4770, 345
RTar	$C_{12}H_{19}NO_8$, 305.28	$P\bar{1}$, 120	a = 7.2647 (5), b = 7.9475 (6), c = 12.5853 (10), α = 77.231 (3), β = 85.330 (5), γ = 79.854 (5), 696.89 (9), 2	27.0, 0.075, 0.639	0.058, 0.113, 1.10, 3037, 226
LMD	$C_{16}H_{19}NO_4$, 289.32	$P2_1$, 123	a = 8.9110 (7), b = 8.3625 (6), c = 9.6575 (8), β = 91.246 (7), 719.49 (10), 2	28.76, 0.036, 0.677	0.036, 0.050, 0.75, 3213, 204
RMD	$C_{16}H_{19}NO_4$, 289.32	$P\bar{1}$, 123	a = 6.4446 (3), b = 10.1143 (5), c = 12.2128 (6), α = 91.239 (4), β = 99.455 (4), γ = 96.794 (4), 779.05 (7), 2	25.99, 0.048, 0.617	0.057, 0.134, 0.94, 3009, 197

3.2. Similarities in cation crystal packing

The 42 salt structures were compared with regard to similarity in cation packing using the 'crystal packing similarity' module in *Mercury* CSD 2.3 (Macrae *et al.*, 2008). This is achieved by taking a reference molecule and then examining the three-dimensional space surrounding that molecule. The resulting cluster of molecules is compared to analogous clusters within all other structures and their geometric similarity is measured. An excellent and thorough description of this technique is given by Childs *et al.* (2009). The analysis was performed by looking solely at the tyrammonium cation, in order to prevent interference from the variable types of anions and different numbers of water molecules also present in the structures.

The tree diagram in Fig. 2 shows the results of the analysis. The diagram was constructed by examining various cluster sizes ranging from two to 15 cations, with a tolerance error of

20% on the distances and torsion angles (Childs *et al.*, 2009). At the bottom of the tree diagram, each independent group forms an isostructural set with 15 out of 15 cations similarly packed in each cluster of the group. Moving from here further up the tree, the similarity in cation packing decreases until the top of the tree where there are six structures that do not have any similarity to each other, or indeed to any of the other structures, in terms of cation packing. The splits in the tree represent similar substructures. The hydrated salts are illustrated by the blue shaded ovals. The small different coloured dots represent the different cation conformations, red is the common extended conformation, blue is the folded conformation and green represents the *m*-toluate structure that contains both the extended and folded cation conformations. Note that all the folded cation-containing structures lie towards the top of the tree, indicating that here a different cation conformation is correlated to different cation packing behaviour.

The tree diagram shows that there are several structures that are isostructural with respect to cation packing, groups 1–6 at the bottom of the tree. Most of the isostructural groups appear to encompass similar anion types, with groups 1, 2 and 3 all containing only anhydrous benzoate salts and group 4 containing hydrated dicarboxylate salts. Groups 5 and 6 are interesting as they contain salts with different anion types and/or variable water content. Note that group 5 contains two anhydrous halide salts and three hydrated salts of inorganic tetrahedral anions. Fig. 3 shows the isostructural packing for the bromide and dihydrogenphosphate salts both with and without the presence of the anions and water molecules. Although the cation packing in both is identical, the anion packing is very different with the bromide ion and the dihydrogenphosphate and two water molecules occupying different positions within the arrangement. Hydrogen bonding is discussed in more detail below, but as most hydrogen bonds involve cation-to-anion interactions or interactions with water molecules, the implication of the different anion and water positions seen in these isostructural groups is that cation packing can be identical even where hydrogen bonding is distinctly different. A similar conclusion was drawn from packing and hydrogen bonding analysis of 37 structures of

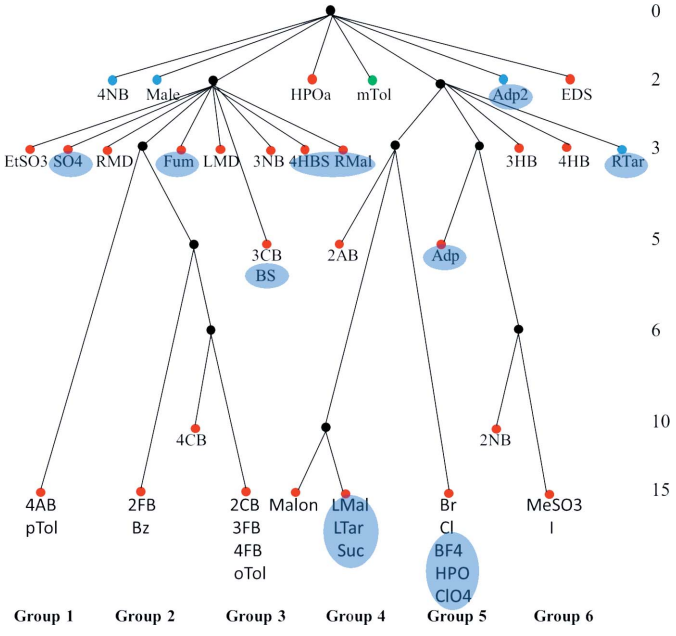

Figure 2
Similarity packing tree diagram for 42 tyrammonium salt structures. The coloured dots represent the different cation conformations, red is the common extended conformation, blue is the folded conformation and green represents the *m*-toluate structure that contains both the extended and folded cation conformations. The hydrated salts are illustrated with blue ovals.

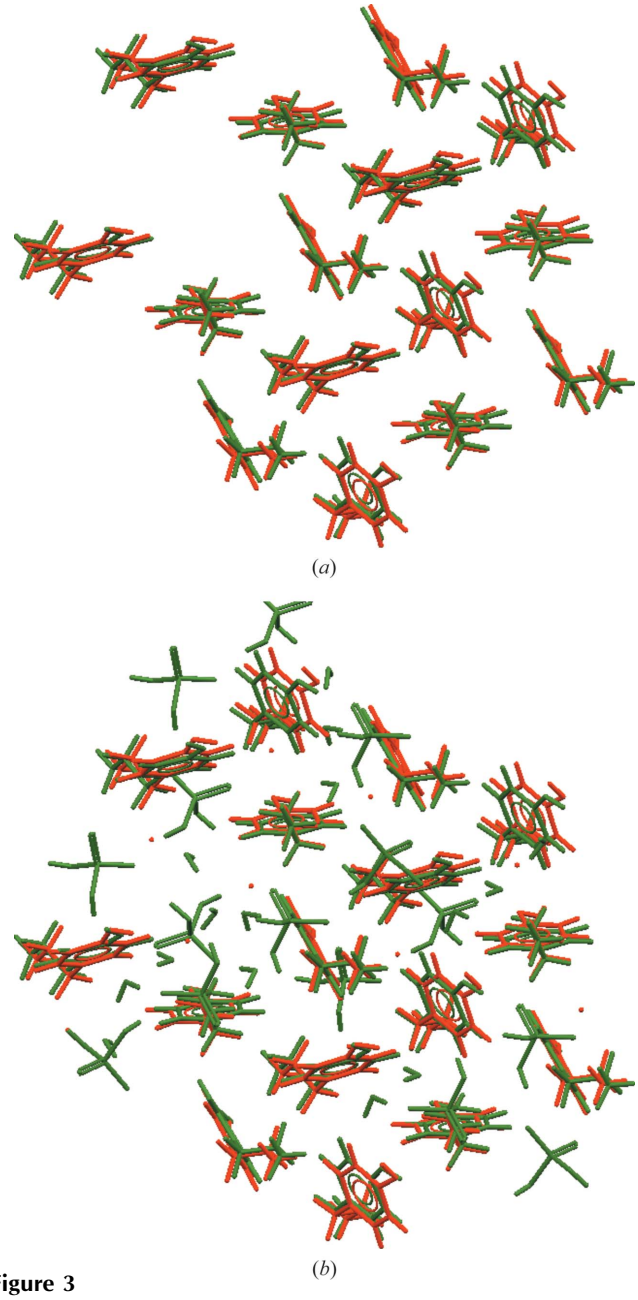

Figure 3
Overlay diagrams showing isostructural packing for group 5 bromide and hydrated dihydrogen phosphate salts. Red represents the bromide salt and green represents the dihydrogen phosphate salt. (*a*) Packing of cations only, and (*b*) all molecules and ions shown.

methylephedrine salts (Kennedy *et al.*, 2011) and a related point is made by Collier *et al.* (2006) who state that it is the amphiphilic nature of the ephedrine cation that dominates structures of its simple salts.

3.3. Benzoate, substituted benzoate and mandelate salts

Salt formation was attempted between tyramine and 19 benzoic acid derivatives as well as with both enantiopure and racemic mandelic acid, see Scheme 2. 20 of these acid–base combinations produced single crystals suitable for analysis by X-ray diffraction. Of these, 19 produced crystals of a desired salt form and one produced crystals of an 'unwanted' product namely the starting material 2-hydroxybenzoic acid. All 19 salts in this section were anhydrous and all the salt structures feature cation-to-anion hydrogen-bond interactions. These species are thus contact ion pairs. The formation of cation-to-cation or anion-to-anion hydrogen bonds is rarer and occurs only in five species – the 3CB, LMD, 4NB, 4HB and 3HB salts. With each tyrammonium cation containing four potential hydrogen-bond donor atoms and one hydrogen-bond acceptor atom, whilst the benzoate and mandelate anions contain at least two hydrogen-bond acceptor atoms and a variety of other functional groups there are a variety of extensive hydrogen-bonding networks present. The hydrogen-bond networks extend in three dimensions for all salts except 2AB, 2NB, mTol, 4NB and RMD, where only two-dimensional networks exist. Interestingly 14 of the 19 structures share two common hydrogen-bonded motifs and it is the five structures highlighted above as being the only ones to form cation-to-cation or anion-to-anion hydrogen bonds that do not share these features. The two common motifs are illustrated in Figs. 4 and 5, and can be described by graph-set notation as $C_2^2(6)$ and $C_2^2(13)$. The first motif utilizes two hydrogen-bond donor atoms of the same $R\mathrm{NH}_3^+$ group to bridge between the carboxylate groups of two anions and forms a chain through the OCO group. The second uses two hydrogen-bond donors at opposite ends of the cation (one NH proton and that of the phenol OH) so that carboxylate groups are bridged by the entire length of the cation. The ladder-like motif observed to be common for other $R\mathrm{NH}_3^+$ salts of carboxylic acids is not observed here (Kinbara *et al.*, 1996).

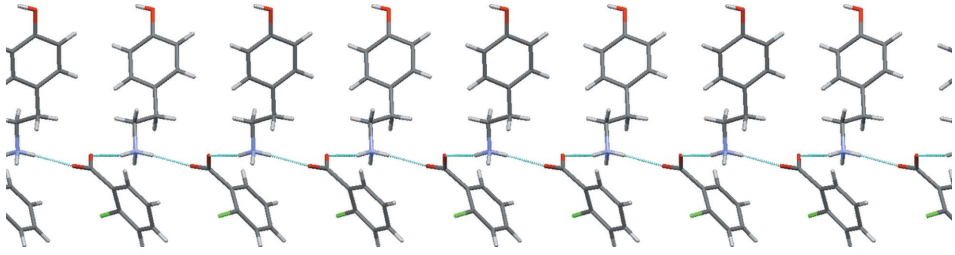

Figure 4
Part of hydrogen-bonded chain illustrating the $C_2^2(6)$ graph set. Here the one-dimensional chain propagates along the crystallographic *c* direction of tyrammonium 2-chlorobenzoate.

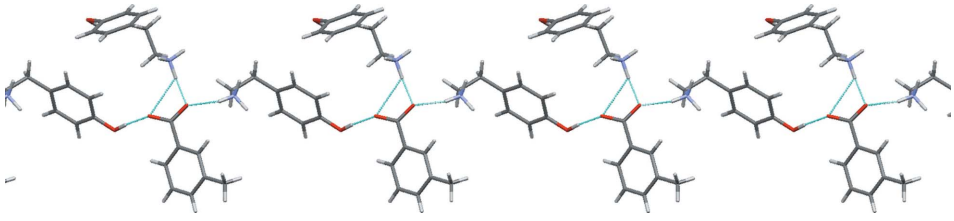

Figure 5
Part of the hydrogen-bonded chain illustrating the $C_2^2(13)$ graph set. Here the one-dimensional chain propagates along the crystallographic *c* direction of tyrammonium *m*-toluate.

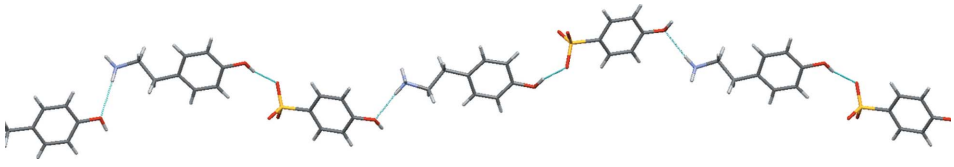

Figure 6
One-dimensional hydrogen-bonded chain propagating along the crystallographic *b* direction through the $C_2^2(17)$ graph set in the structure of tyrammonium 4-hydroxybenzenesulfonate hemihydrate.

3.4. Sulfonate salts

There are five structures available of tyrammonium salts of organic sulfonates; the three aliphatic species $\mathrm{MeSO_3}$, $\mathrm{EtSO_3}$ and EDS (ethylenedisulfonate) and the two benzene derivatives are hydrated salts (the benzenesulfonate is a monohydrate and the 4-hydroxybenzenesulfonate is a hemihydrate). All five salts form three-dimensional hydrogen-bonded networks and all feature a $C_2^2(6)$ hydrogen-bonding motif which is equivalent to that shown for the carboxylate species in Fig. 4. The $C_2^2(13)$ graph-set seen for most of the benzoate salts is also present in four out of the five sulfonate structures. The exception is the 4-hydroxybenzenesulfonate salt which adopts a $C_2^2(17)$ motif. This encompasses the lengths of both the cations and the anions as shown in Fig. 6. As with the benzoate group of structures, this one exceptional structure is the only one of the sulfonate group to feature a cation-to-cation hydrogen bond.

3.5. Halide salts

Salt synthesis was successful for the chloride, bromide and iodide salts of tyramine. As with the benzoate derived salts all three halide species are anhydrous. The chloride and iodide structures were already available in the literature

(Podder *et al.*, 1979; Ivanova & Spiteller, 2010). The chloride and bromide salts are isostructural with only a slight increase in the unit cell size to accommodate the larger bromide anion, see Fig. 7. All three halide structures form three-dimensional hydrogen-bonded networks containing a $C_2^1(11)$ graph-set motif. This is analogous to the $C_2^2(13)$ graph set seen for the benzoate and sulfonate based salts above, with a one-atom halide fragment taking the place of the three-atom OCO or OSO units in the larger motif, illustrated by Fig. 5.

3.6. Tetrahedral anions

There are five salts in the dataset formed from tetrahedral anions of the general type AX_4. These are tetrafluoroborate (BF4), perchlorate (ClO4), dihydrogenphosphate (HPO and HPOa) and sulfonate (SO4) salts. Crystallization of the dihydrogenphosphate salt in a methanol:acetonitrile medium reportedly produced an anhydrous dihydrogenphosphate salt (HPOa; Kolev *et al.*, 2009). However, in our hands and in an aqueous medium all four anions produced hydrated salt species. BF4 and ClO4 are both monohydrates, and HPO is a dihydrate. Despite differences in hydration state and the obvious differences in hydrogen-bonding potential of the anions, three of these salts are isostructural with respect to cation packing as is shown by their presence in group five of the isostructural tree, see Fig. 2. The sulfate salt structure by necessity differs as the sulfate is a dianion, and thus there is a difference in the cation-to-anion ratio.

All five salts of the tetrahedral anions form three-dimensional networks through hydrogen bonding. The variable number of water molecules and the nature of the anions gives complicated graph-set analyses, however, the common $C_2^1(11)$ motif seen within the halide structures is present for the HPO and SO4 salts. An interesting feature is the $C_2^1(11)$ motif illustrated in Fig. 8. Similar features are common throughout the other salts (see Fig. 5) – but they always involve chains of cations and anions. Here water has taken over the hydrogen-bonding role of the anion.

3.7. Dicarboxylate salts

There are ten dicarboxylate structures available for analysis, two are anhydrous and eight are hydrate species. With the potential for one- or twofold deprotonation, the ratio of cation-to-anion varies throughout the structures. There are four one-to-one salts and four two-to-one salts as well as two co-crystals, both of which feature two cations per doubly deprotonated anion in the presence of one free acid molecule. There are multiple available hydrogen-bond donor and acceptor atoms resulting in extensive hydrogen-bonding networks and so two of the salts form two-dimensional sheets and the other eight salts form three-dimensional hydrogen-bonded networks. Table 2 summarizes the gross structural features and hydrogen-bond interactions found for these species. Both anhydrous species are composed of a salt with a singly deprotonated acid and with only one hydrogen-bond donor atom present on the anion. In the case of the hydrogen-maleate structure this hydrogen bond donor forms a typical intramolecular bond resulting in a $S_1^1(7)$ graph set. This reduces the number of hydrogen-bond donors available and may thus explain the formation of a two-dimensional sheet instead of the more common three-dimensional hydrogen-bonded network. Interestingly, the hydrogen malonate anion does not have an intramolecular hydrogen bond as is normally found elsewhere (Kennedy *et al.*, 2011; Saraswathi & Vijayan,

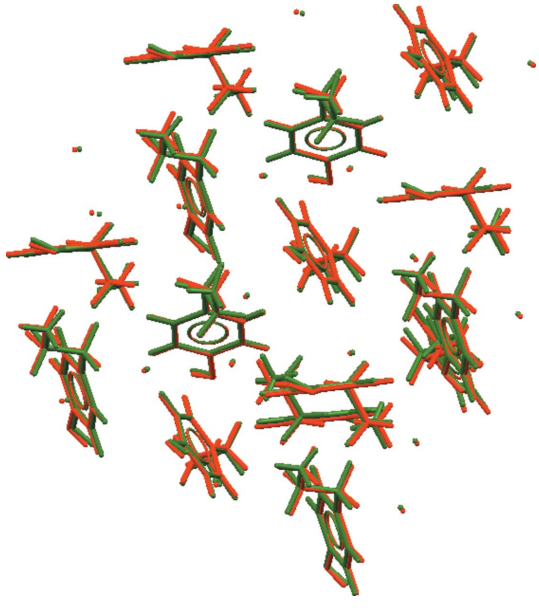

Figure 7
Isostructural packing of cations and anions in chloride and bromide salts. Green represents the chloride salt and red represents the bromide salt.

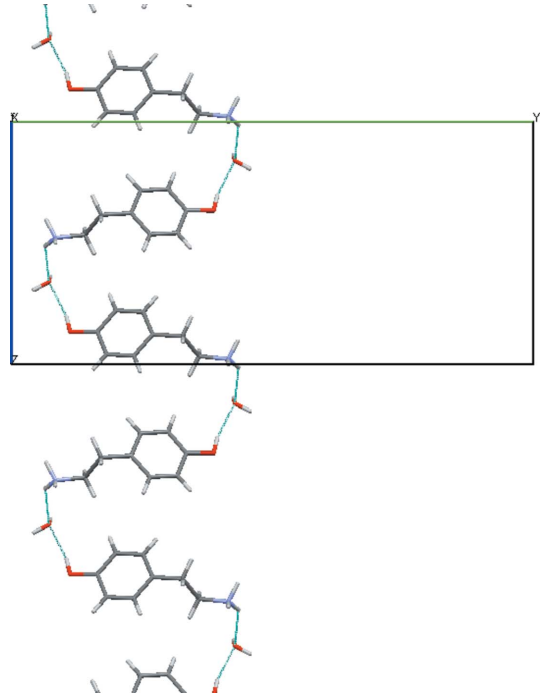

Figure 8
Hydrogen-bonded chain found in the ClO4 and BF4 salts.

Table 2
Summary of the composition and main structural features found for the dicarboxylate salt structures.

C = cation, *A* = anion and *W* = water.

	Unit-cell contents				Hydrogen-bond interactions								
Salt	Cation	Anion	Free acid	Water	*C*···*A*	*A*···*C*	*C*···*C*	*A*···*A*	*C*···*W*	*W*···*C*	*A*···*W*	*W*···*A*	Hydrogen-bond network
Male	1	1	–	–	X	N/a	X	Intra	N/a	N/a	N/a	N/a	Two-dimensional
Malon	1	1	–	–	X	–	X	X	N/a	N/a	N/a	N/a	Three-dimensional
RMal	1	1	–	1	X	–	–	X	X	–	X	X	Three-dimensional
RTar	1	1	–	1	X	–	–	X	–	–	X	X	Three-dimensional
Apd2	1	0.5	–	1	X	N/a	X	N/a	X	–	N/a	X	Two-dimensional
Suc	1	0.5	–	1	X	N/a	–	N/a	X	–	–	X	Three-dimensional
LMal	1	0.5	–	1	X	X	–	–	X	–	–	X	Three-dimensional
LTar	1	0.5	–	1	X	X	X	X	X	–	–	X	Three-dimensional
Adp	1	0.5	0.5	0.25	X	X	–	X	X	X	–	X	Three-dimensional
Fum	1	0.5	0.5	1	X	–	X	X	X	–	–	X	Three-dimensional

2002; Hemamalini *et al.*, 2004; Eppel & Bernstein, 2009; Sarma *et al.*, 2011). Instead the less common (and intermolecular hydrogen-bond forming) *anti* conformation is observed (for other examples see Djinović & Golič, 1991; Wu & Wu, 2010). Despite this difference, the hydrogen malonate still gives an anhydrous species. The two enantiopure racemic pairs both give chemically different species for the racemates (isolated as hydrogen tartrate and hydrogen malate) as opposed to the enantiopure forms (both isolated as dideprotonated anions). The two enantiopure salts and the succinate salt are isostructural with respect to cation packing and are located in group four of the isostructural tree, see Fig. 2. Additionally, the two enantiopure salts are also nearly isostructural with respect to their anion and water packing as well, see Fig. 9.

3.8. Environment of water molecules

Hydrated salts formed for one third of the 42 salts, an occurrence rate substantially above those observed in literature studies based on the CSD, including that found in a study of NH^+-containing salts of pharmaceutically acceptable counterions (Haynes *et al.*, 2005). Within these 14 structures there are 19 crystallographically independent water molecules that each have one of two different water environments. Thus, water acts as a two-hydrogen-bond donor, one-hydrogen-bond acceptor molecule or as a two-hydrogen-bond donor, two-hydrogen-bond acceptor molecule, see examples in Fig. 10. The first is the most common environment occurring for 12 of the water molecules, and the latter occurs for seven of the water molecules. These results agree with a study of hydrates which found that the most common solid-state environments for water molecules were those where three or four hydrogen bonds were present between water and its neighbouring molecules (Gillon *et al.*, 2003).

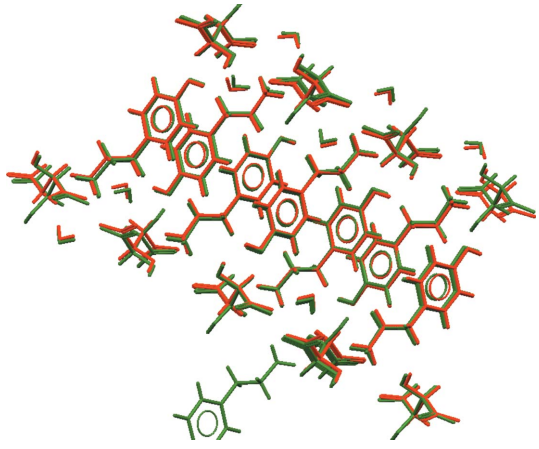

Figure 9
Isostructural packing of cations, anions and water molecules for L-maleate and L-tartrate salts

3.9. Predicting the formation of a hydrate

From the above category based analysis of the structures, there are some obvious trends for hydrate formation. The following rules for predicting the formation of hydrates of tyrammonium salts can thus be proposed.

(i) All benzoate and halide anions form anhydrous salts.

(ii) All tetrahedral anions form hydrated salts, when crystallized from an aqueous environment.

(iii) Aliphatic sulfonate anions give anhydrous salts whilst aryl-sulfonates form hydrated salts, although the numbers of examples for these two categories are low.

(iv) All the dicarboxylate-based anions form hydrated salts, unless their anion has the ability to form an intramolecular hydrogen bond.

Examining these 'chemical-category'-based rules suggests that hydrate formation is achieved when there are larger numbers of hydrogen-bond donor and/or acceptor atoms present, as seen with the tetrahedral and dicarboxylate salts. This observation agrees with the literature, where it has been suggested that the occurrence of hydrates generally rises with an increasing number of polar groups on a molecule and with increasing charge (Infantes *et al.*, 2003).

3.10. Donor:acceptor ratios

Following the guidelines of Etter's rules (Etter, 1990) which state that all good hydrogen-bond donor and acceptor atoms will be involved in hydrogen bonding, there has been much debate within the literature as to whether hydrate formation is

linked to hydrogen-bond donor:acceptor ratios. A study by Desiraju (1991) concluded that the inclusion of water helps stabilize compounds where there is an imbalance of hydrogen-bond donor and acceptor atoms present – and it is implied that water does this by providing 'extra' donor atoms to donor-deficient species. Infantes *et al.* (2007) contradict this statement and state that their studies showed no link between hydrate formation and donor:acceptor ratios, instead they propose a link between hydrate formation and the sum of the donor and acceptor counts for functional groups along with an increased polar surface area. In the current paper there are 41 salts of tyramine isolated from aqueous media (the exception is the anhydrous salt HPOa which was crystallized from a methanol:acetonitrile medium by Kolev *et al.*, 2009). Hydrogen-bond donor:acceptor ratios were calculated for these 41 salts to see if this ratio has any detectable influence on the rate of occurrence of hydrate formation.

Donor:acceptor ratios were calculated in several different ways. First a calculation that assumed no prior knowledge of the crystal structure was performed. All acids were assumed to form a tyramine salt with a one-to-one ratio of cations to anions (*e.g.* acids with two ionisable protons were assumed to form monodeprotonated species such as hydrogen tartrate). Ratios were also calculated for the actual observed contents of the asymmetric unit and this was done both with water molecules ignored and with the observed hydrogen bonding of the water molecules included. Results for these three sets of calculations are shown in Fig. 11. These results indicate that it is not possible to absolutely predict hydrate formation from examining the cation and anion donor:acceptor ratio alone. However, hydrate formation does appear to be more likely with an increase in the number of hydrogen-bond acceptors (and hence lower ratios). As water primarily occurs in the structures where there is an excess of hydrogen-bond acceptors, this could indicate that here the primary structural role of water molecules is to provide extra hydrogen-bond donors. This fits with the observed tendency, described above, of water to make more donor interactions than it does acceptor interactions. This observation with respect to acceptor:donor ratios also fits with the earlier comment that the tetrahedral, sulfonate and dicarboxylate salt categories have high occurrences of hydrate formation. All these anion types have high numbers of hydrogen-bond acceptor atoms and relatively few donor atoms.

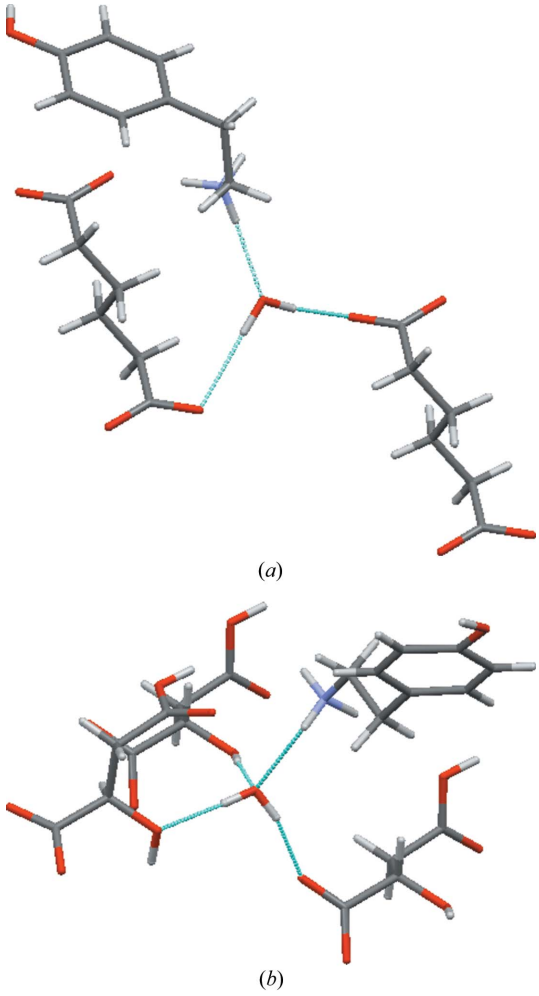

Figure 10
Water environments; (*a*) two donor, one acceptor (Adp2) or (*b*) two donor, two acceptor (RMal).

Moving away from ratios and simply calculating the total numbers of acceptor and donor atoms (as per Infantes *et al.*, 2007) gives a range of 8 to 14 (acceptor + donor) atoms for the hydrates and 6 to 12 (acceptor + donor) atoms for the anhydrates (averages 11.29 and 7.81). As the two ranges overlap there is again no absolute prediction of hydrate formation available here. However, we do find that as stated by Infantes *et al.* (2007) there is an increased likelihood of hydrate formation with increased numbers of (acceptor + donor) atoms. Where the current work differs from that of Infantes *et al.* (2007) and instead agrees with the earlier work of Desiraju (1991) is that a correlation with donor:acceptor ratios is also observed. The obvious difference in methodology between the current work and that of Infantes *et al.* is that this work looks at a tightly knit family of related salt structures, all of which were crystallized from water, whilst the Infantes work reviewed a much wider range of organic structures drawn from the CDS. To bring the two works together it is thus suggested that donor:acceptor ratios do influence the rate of occurrence of hydrate formation, but perhaps this effect can only be observed where variability in chemical type is restricted.

4. Conclusion

This study describes 38 new structures of salts of the PEA base tyramine. It finds that the tyrammonium cation normally adopts an extended conformation but that a folded conformation also exists. Analysis of the cation–cation packing finds several isostructural groupings and two of these groups are flexible enough to allow large variations in anion type, water content and hydrogen bonding. This suggests that cation-to-cation packing may have a greater role to play in influencing the final structure adopted than hydrogen bonding. Analysis of the likelihood of hydrate formation shows that certain

anion types (benzoates, halides) give anhydrous salt forms whilst others (dicarboxylate and tetrahedral AX_4 anions) tend to give hydrated species. The prior observation of Infantes *et al.* (2007) that species with higher total numbers of potential hydrogen-bond acceptor and donor atoms are more likely to form hydrates is confirmed. However, contrary to the findings of Infantes *et al.* but in agreement with those of Desiraju (1991), it is also found that analysis of acceptor:donor ratios indicates that donor-deficient species are more likely to form hydrates.

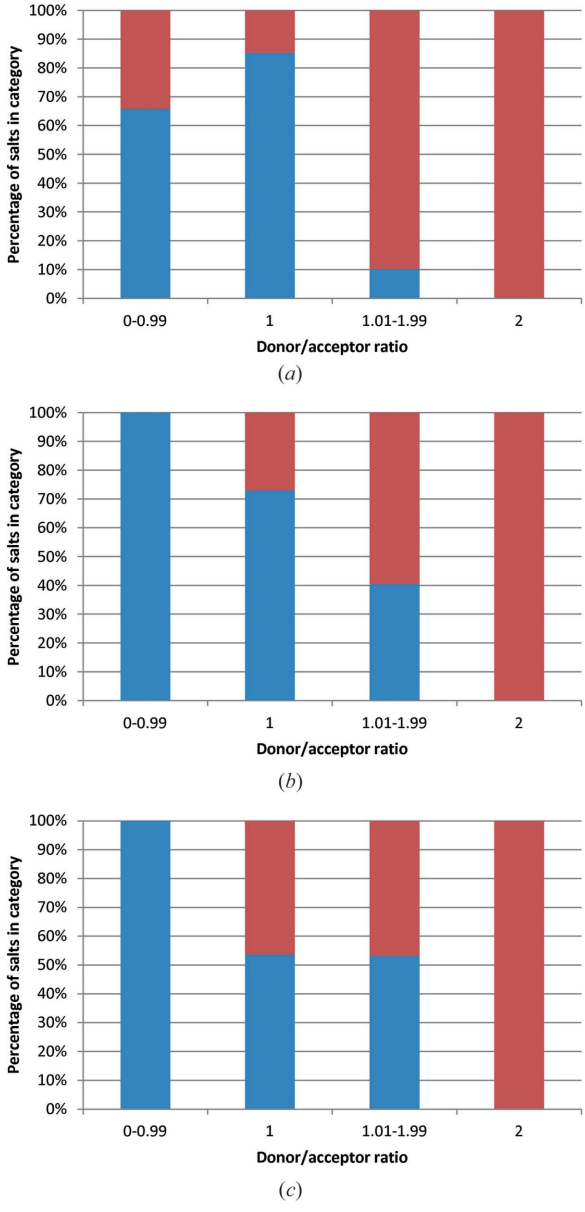

Figure 11
Donor:acceptor ratios calculated: (*a*) assuming no water present and the presence of only one cation and one anion per formula unit; (*b*) for the contents of the asymmetric unit with water disregarded; (*c*) for the contents of the asymmetric unit including the observed acceptor–donor behaviour of water molecules. Hydrated salts are blue, anhydrous salts are red.

The authors thank the University of Strathclyde and MSD for funding a studentship (CAM) and the National Crystallography Service staff of the Universities of Southampton and Newcastle for five data collections.

References

Altomare, A., Burla, M. C., Camalli, M., Cascarano, G. L., Giacovazzo, C., Guagliardi, A., Moliterni, A. G. G., Polidori, G. & Spagna, R. (1999). *J. Appl. Cryst.* **32**, 115–119.

Altomare, A., Cascarano, G., Giacovazzo, C., Guagliardi, A., Burla, M. C., Polidori, G. & Camalli, M. (1994). *J. Appl. Cryst.* **27**, 435.

Arlin, J. B., Florence, A. J., Johnston, A., Kennedy, A. R., Miller, G. J. & Patterson, K. (2011). *Cryst. Growth Des.* **11**, 1318–1327.

Black, S. N., Collier, E. A., Davey, R. J. & Roberts, R. J. (2007). *J. Pharm. Sci.* **96**, 1053–1068.

Bruker AXS Inc. (2007). *SAINT* and *SADABS*. Bruker AXS Inc., Madison, Wisconsin, USA.

Childs, S. L., Wood, P. A., Rodriguez-Hornedo, N., Reddy, L. S. & Hardcastle, K. I. (2009). *Cryst. Growth Des.* **9**, 1869–1888.

Clarke, H. D., Arora, K. K., Bass, H., Kavuru, P., Ong, T. T., Pujari, T., Wojtas, L. & Zaworotko, M. J. (2010). *Cryst. Growth Des.* **10**, 2152–2167.

Cole, S. J. & Gale, P. A. (2012). *Chem. Sci.* **3**, 683–689.

Collier, E. A., Davey, R. J., Black, S. N. & Roberts, R. J. (2006). *Acta Cryst.* B**62**, 498–505.

D'Andrea, G., Nordera, G. P., Perini, F., Allais, G. & Granella, F. (2007). *Neurol. Sci*, **28**, s94–s96.

Desiraju, G. R. (1991). *J. Chem. Soc. Chem. Commun.* pp. 426–428.

Djinović, K. & Golič, L. (1991). *Acta Cryst.* C**47**, 2367–2371.

Duddu, S. P. & Grant, D. J. (1994). *Pharm. Res.* **11**, 1549–1556.

Eppel, S. & Bernstein, J. (2009). *Cryst. Growth Des.* **9**, 1683–1691.

Etter, M. C. (1990). *Acc. Chem. Res.* **23**, 120–126.

Farrugia, L. J. (1997). *J. Appl. Cryst.* **30**, 565.

Gillon, A. L., Feeder, N., Davey, R. J. & Storey, R. (2003). *Cryst. Growth Des.* **3**, 663–673.

Görbitz, C. H. & Hersleth, H.-P. (2000). *Acta Cryst.* B**56**, 526–534.

Gould, P. L. (1986). *Int. J. Pharm.* **33**, 201–217.

Grant, D. J. W. & Higuchi, T. (1990). *Solubility Behaviour of Organic Compounds.* New York: Wiley.

Haynes, D. A., Jones, W. & Motherwell, W. D. S. (2005). *CrystEngComm*, **7**, 342–345.

Hemamalini, M., Muthiah, P. T. & Butcher, R. J. (2004). *Acta Cryst.* E**60**, o2350–o2352.

Infantes, L., Chisholm, J. & Motherwell, S. (2003). *CrystEngComm*, **5**, 480–486.

Infantes, L., Fabian, L. & Motherwell, W. D. S. (2007). *CrystEngComm*, **9**, 65–71.

Infantes, L. & Motherwell, W. D. S. (2002). *CrystEngComm*, **4**, 454–461.

Ivanova, B. & Spiteller, M. (2010). *Spectrochim. Acta Part A*, **77**, 849–855.

Kennedy, A. R., Andrikopoulos, P. C., Arlin, J. B., Armstrong, D. R., Duxbury, N., Graham, D. V. & Kirkhouse, J. B. (2009). *Chem. Eur. J.* **15**, 9494–9504.

Kennedy, A. R., Kirkhouse, J. B., McCarney, K. M., Puissegur, O., Smith, W. E., Staunton, E., Teat, S. J., Cherryman, J. C. & James, R. (2004). *Chem. Eur. J.* **10**, 4606–4615.

Kennedy, A. R., Morrison, C. A., Briggs, N. E. B. & Arbuckle, W. (2011). *Cryst. Growth Des.* **11**, 1821–1834.

Kennedy, A. R., Okoth, M. O., Sheen, D. B., Sherwood, J. N., Teat, S. J. & Vrcelj, R. M. (2003). *Acta Cryst.* C**59**, o650–o652.

Khankari, R. K. & Grant, D. J. W. (1995). *Thermochim. Acta*, **248**, 61–79.

Kiang, Y. H., Xu, W., Stephens, P. W., Ball, R. G. & Yasuda, N. (2009). *Cryst. Growth Des.* **9**, 1833–1843.
Kinbara, K., Hashimoto, Y., Sukegawa, M., Nohira, H. & Saigo, K. (1996). *J. Am. Chem. Soc.* **118**, 3442–3449.
Koleva, B. B., Kolev, T., Seidel, R. W., Spiteller, M., Mayer-Figge, H. & Sheldrick, W. S. (2008). *J. Mol. Struct.* **888**, 138–144.
Kolev, T. M., Koleva, B. B., Spiteller, M., Sheldrick, W. S. & Mayer-Figge, H. (2009). *Amino Acids*, **36**, 185–193.
Lewis, G. R., Steele, G., McBride, L., Florence, A. J., Kennedy, A. R., Shankland, N., David, W. I. F., Shankland, K. & Teat, S. J. (2005). *Cryst. Growth Des.* **5**, 427–438.
Li, Z. J., Ojala, W. H. & Grant, D. J. (2001). *J. Pharm. Sci.* **90**, 1523–1539.
Macrae, C. F., Bruno, I. J., Chisholm, J. A., Edgington, P. R., McCabe, P., Pidcock, E., Rodriguez-Monge, L., Taylor, R., van de Streek, J. & Wood, P. A. (2008). *J. Appl. Cryst.* **41**, 466–470.
Morris, K. (2009). In *Structural Aspect of Hydrates and Solvates*, 2nd ed. New York: Informa Healthcare.
Oxford Diffraction (2006). *CrysAlis Pro.* Oxford Diffraction Ltd, Abingdon, England.
Podder, A., Dattagupta, J. K., Saha, N. N. & Saenger, W. (1979). *Acta Cryst.* B**35**, 649–652.
Rigaku Corporation (2008). *CrystalClear.* Rigaku Corporation, The Woodlands, Texas, USA.
Saraswathi, N. T. & Vijayan, M. (2002). *Acta Cryst.* B**58**, 1051–1056.
Sarma, B. S. B., Thakuria, R., Nath, N. K. & Nangia, A. (2011). *CrystEngComm*, **13**, 3232–3240.
Shankland, N., David, W. I. F., Shankland, K., Kennedy, A. R., Frampton, C. S. & Florence, A. J. (2001). *Chem. Commun.* pp. 2204–2205.
Sheldrick, G. M. (2008). *Acta Cryst.* A**64**, 112–122.
Siddiqui, S. A., Dwivedi, A., Singh, P. K., Hasan, T., Jain, S., Sundaraganesan, N., Saleem, H. & Misra, N. (2009). *J. Theor. Comput. Chem.* **8**, 433–450.
Spek, A. L. (2003). *J. Appl. Cryst.* **36**, 7–13.
Stahl, P. H. (1980). *Towards Better Safety of Drugs and Pharmaceutical Products.* Amsterdam: Elsevier/North-Holland Biomedical Press.
Stahl, P. H. & Wermuth, C. G. (2008). *Handbook of Pharmaceutical Salts: Properties, Selection and Uses.* Zurich: VHCA.
Vippagunta, S. R., Brittain, H. G. & Grant, D. J. W. (2001). *Adv. Drug Deliv. Rev.* **48**, 3–26.
Wu, D.-H. & Wu, Q.-Q. (2010). *Acta Cryst.* E**66**, o2160.